Neurochemistry International 124 (2019) 171–180

Contents lists available at ScienceDirect

Neurochemistry International

journal homepage: www.elsevier.com/locate/neuint

The effects of zonisamide on L-DOPA–induced dyskinesia in Parkinson's disease model mice

Hiromi Sano[a,b], Atsushi Nambu[a,b,*]

[a] Division of System Neurophysiology, National Institute for Physiological Sciences, 38, Nishigonaka, Myodaiji, Okazaki, Aichi, 444-8585, Japan
[b] Department of Physiological Sciences, SOKENDAI (The Graduate University for Advanced Studies), 38, Nishigonaka, Myodaiji, Okazaki, Aichi, 444-8585, Japan

ARTICLE INFO

Keywords:
Parkinson's disease
Zonisamide
L-DOPA–induced dyskinesia
Basal ganglia

ABSTRACT

Parkinson's disease (PD) is a neurodegenerative disorder caused by the loss of dopaminergic neurons in the midbrain and shows motor dysfunctions. Zonisamide (ZNS, 1,2-benzisoxazole-3-methanesulfonamide), which was originally developed as an antiepileptic drug, was also found to have beneficial effects on motor symptoms in PD. In the current study, we have investigated the behavioral and physiological effects of ZNS on L-DOPA–induced dyskinesia (LID) in PD model mice. Chronic administration of L-DOPA plus ZNS in PD model mice was shown to increase the duration and severity of LID compared with PD model mice that were treated with L-DOPA alone. To elucidate the neural mechanism of the effects of ZNS on LID, we examined neuronal activity in the output nuclei of the basal ganglia, i.e., the substantia nigra pars reticulata (SNr). Chronic administration of L-DOPA plus ZNS in PD mice decreased the firing rate in the SNr while they showed apparent LID. In addition, chronic treatment of L-DOPA plus ZNS in PD mice changed cortically evoked responses in the SNr during LID. In the control state, motor cortical stimulation induces the triphasic response composed of early excitation, inhibition, and late excitation. In contrast, L-DOPA plus ZNS–treated PD mice showed longer inhibition and reduced late excitation. Previous studies proposed that inhibition in the SNr is derived from the *direct* pathway and releases movements, and that late excitation is derived from the *indirect* pathway and stops movements. These changes of the *direct* and *indirect* pathways possibly underlie the effects of ZNS on LID.

1. Introduction

Parkinson's disease (PD) is a progressive neurodegenerative disorder caused by the loss of nigrostriatal dopaminergic neurons in the substantia nigra pars compacta (SNc). PD symptoms are characterized by tremor at rest, rigidity, akinesia (or bradykinesia), postural instability, and non-motor disorders (Jankovic, 2008). In the widely accepted model of the basal ganglia, the *direct* and *indirect* pathways are functionally opposed (Alexander and Crutcher, 1990). In the *direct* pathway, striatal projection neurons directly inhibit the output nuclei of the basal ganglia (i.e., the substantia nigra pars reticulata [SNr] and the entopeduncular nucleus [EPN]), disinhibit the thalamus, and facilitate movements. On the other hand, in the *indirect* pathway, striatal projection neurons project polysynaptically to the SNr/EPN through the external segment of the globus pallidus (GPe) and subthalamic nucleus (STN), activate the SNr/EPN, inhibit the thalamus, and decrease movements. In the healthy state, the *direct* and *indirect* pathways are supposed to be balanced. According to the classical model of PD, loss of nigrostriatal dopaminergic neurons leads to underactivity of the *direct* pathway striatal projection neurons through excitatory dopamine D1 receptors and overactivity of the *indirect* pathway striatal projection neurons through inhibitory D2 receptors. Administration of L-3,4-dihydroxyphenylalanine (L-DOPA) as dopamine replacement therapy ameliorates PD symptoms and remains the standard therapy for PD. However, long-term administration of L-DOPA induces the emergence of abnormal involuntary movements, i.e., L-DOPA–induced dyskinesia (LID). The classical explanation for LID is that changes in the *direct* and *indirect* pathways occur in the directions opposite to that of PD (Jenner,

Abbreviations: 6-OHDA, 6-hydroxydopamine; AIMs, abnormal involuntary movements; CV, coefficient of variation; EPN, entopeduncular nucleus; GPe, external segment of the globus pallidus; GPi, internal segment of the globus pallidus; ISIs, interspike intervals; LID, L-DOPA–induced dyskinesia; MPTP, 1-methyl-4-phenyl-1,2,3,6-tetrahydropyridine; PD, Parkinson's disease; PBS, phosphate-buffered saline; SNc, substantia nigra pars compacta; SNr, substantia nigra pars reticulata; STN, subthalamic nucleus; TH, tyrosine hydroxylase; ZNS, zonisamide (1,2-benzisoxazole-3-methanesulfonamide)

* Corresponding author. Division of System Neurophysiology, National Institute for Physiological Sciences, 38, Nishigonaka, Myodaiji, Okazaki, Aichi, 444-8585, Japan.
E-mail address: nambu@nips.ac.jp (A. Nambu).

https://doi.org/10.1016/j.neuint.2019.01.011
Received 30 October 2018; Received in revised form 9 January 2019; Accepted 9 January 2019
Available online 11 January 2019

2008). L-DOPA overstimulates the D1 and D2 receptors in the striatal neurons and thereby induces overactivity of the *direct* pathway and underactivity of the *indirect* pathway.

Zonisamide (ZNS, 1,2-benzisoxazole-3-methanesulfonamide) was developed as an antiepileptic drug with more effective anticonvulsant and has been used to treat epilepsy (Peters and Sorkin, 1993; Seino, 2004). Incidentally, it was also found to have beneficial effects on PD symptoms (Murata et al., 2001, 2007; Murata, 2004) and was approved as adjunctive therapy for PD in Japan. ZNS lessens PD symptoms such as wearing-off (Murata et al., 2015), tremor, rigidity, and bradykinesia. Although the mechanism of ZNS on PD is not fully elucidated, it is known that ZNS has multiple mechanisms of action, including inhibition of Na^+ channels (Sobieszek et al., 2003), reduction of T-type Ca^{2+} currents (Kito et al., 1996; Suzuki et al., 1992), and alteration of dopamine metabolism (Okada et al., 1995). It has also shown attenuation of cell death by seizure and ischemia and has indicated neuroprotective effects on nigrostriatal dopaminergic neurons both in genetic PD model mice (Sano et al., 2015) and PD model mice treated by dopaminergic neurotoxins such as 6-hydroxydopamine (6-OHDA) or 1-methyl-4-phenyl-1,2,3,6-tetrahydropyridine (MPTP) (Asanuma et al., 2010; Choudhury et al., 2010; Yano et al., 2009). In addition, ZNS is reported not only to ameliorate LID in PD model rats (Oki et al., 2017), but also not to have negative effect on dyskinesia in patients with PD (Murata et al., 2007, 2015).

To evaluate the effects of ZNS on LID, we used 6-OHDA to generate PD model mice and administered L-DOPA or combined L-DOPA and ZNS to induce LID. Abnormal involuntary movements (AIMs) scores showed that the duration and severity of LID were increased in L-DOPA plus ZNS–treated PD model mice compared to mice treated with L-DOPA alone. To investigate the neural mechanism of ZNS on LID, we recorded neuronal activity in the basal ganglia of L-DOPA plus ZNS (L-DOPA + ZNS)–treated PD model mice under awake conditions. The firing rate of SNr neurons was decreased in L-DOPA + ZNS–treated PD model mice when they clearly showed LID. This effect is possibly related to involuntary movements in LID. We also recorded cortically evoked responses in the basal ganglia to analyze the information flow through the basal ganglia. The responses derived from the *direct* pathway were increased and those from the *indirect* pathway were decreased in L-DOPA + ZNS–treated PD model mice. These changes in response patterns may underlie the mechanism that causes the combination of L-DOPA + ZNS to induce more severe and longer LID.

2. Materials and methods

2.1. Animals

Male ICR mice were purchased from Japan SLC, and each mouse was trained to be habituated to handling by humans. All of the mice used in the experiments were more than 12 weeks old. The mice were maintained in a 12 h light/dark cycle with access to food and water *ad libitum*. The experimental procedures were approved by the Institutional Animal Care and Use Committee of National Institutes of Natural Sciences.

2.2. Experimental design

The timeline of the experiments is shown in Fig. 1A. Mice received 6-OHDA or vehicle in the right medial forebrain bundle, and then the dopaminergic lesion was evaluated by the cylinder test. After 10 days of treatment with chronic saline, L-DOPA, or L-DOPA + ZNS, dyskinetic behaviors were evaluated. Electrophysiological recordings were performed about 24 h after the daily corresponding treatment (saline or L-DOPA + ZNS). After recordings in the GPe and SNr, mice received a daily injection of L-DOPA + ZNS and recordings of the GPe and SNr neurons were performed again from 20 to 120 min after drug treatment. After the final electrophysiological experiment, several sites of recording were marked, then the mice were perfused transcardially and histological analyses were performed. The numbers of animals in each group were as follows: control (n = 3), PD (n = 6), L-DOPA (n = 13), and L-DOPA + ZNS (n = 7).

2.3. 6-OHDA lesions

Desipramine hydrochloride (25 mg/kg, *i.p.*; Sigma-Aldrich) was administered to mice 30 min before 6-OHDA or vehicle infusion. Each mouse was anesthetized with isoflurane (1.0–1.5%) and fixed in the stereotaxic apparatus. 6-OHDA-hidrobromide (4 mg/ml; Sigma-Aldrich or TOCRIS) was dissolved in saline containing 0.02% ascorbic acid. A glass micropipette was connected to a Hamilton microsyringe. The glass micropipette was inserted into one site in the right medial forebrain bundle at the following coordinates, according to the mouse brain atlas (Franklin and Paxinos, 2013): anterior −1.2 mm, lateral 1.2 mm, and ventral 4.8 mm. 6-OHDA solution or vehicle was then injected (1 µl, at 0.2 µl/min) with a microinfusion pump (Micro4, WPI). The mice were allowed to recover for 2 or 3 weeks before behavioral evaluation and chronic L-DOPA treatment.

2.4. Chronic L-DOPA or L-DOPA + ZNS treatment

The 6-OHDA-lesioned mice were treated daily with L-DOPA or L-DOPA + ZNS. L-DOPA was administered (20 mg/kg, *i.p.*; Ohara Pharmaceutical Co., Ltd.) once daily in combination with benserazide (12 mg/kg, *i.p.*; Sigma-Aldrich). For L-DOPA + ZNS, ZNS (100 mg/kg, *i.p.*; provided by Sumitomo Dainippon Pharma Co., LTD) was administered 10 min after L-DOPA treatment. This dosage of ZNS was set based on our previous study (Sano et al., 2015). Non-lesioned and 6-OHDA-lesioned mice were also treated daily with saline (*i.p.)* and were described as 'control' and 'PD', respectively (Fig. 1A).

2.5. Behavioral tests

On day 1 before the first treatment with L-DOPA, L-DOPA + ZNS, or saline, the cylinder test (Meredith and Kang, 2006; Schallert T et al., 2000; Tillerson JL et al., 2001) was performed to evaluate a unilateral lesion of the nigrostriatal dopaminergic neurons induced by 6-OHDA. In brief, each mouse was placed in a clear acrylic cylinder (10 cm diameter and 20 cm height) and video recorded for 5 min without previous habituation to the cylinder. The mice showed an exploratory behavior by rearing and leaning on the wall of the cylinder with their forelimbs. The number of contacts with their right or left forelimb was counted. A limb use asymmetry score was calculated by the number of wall contacts performed with the left forelimb (the forelimb contralateral to the lesion) as percentage of the total wall contacts. If mice showed no impairment in the left forelimb compared to the right forelimb, additional injections of 6-OHDA was performed. On day 10 of chronic treatment with L-DOPA, L-DOPA + ZNS, or saline, LID was scored based on the abnormal involuntary movements (AIMs) scale (Lundblad et al., 2002, 2003, 2004, 2005). AIMs were classified into four subtypes: locomotive (increased locomotion with contralateral rotations), axial (contralateral dystonic posture of the neck and upper body towards the side contralateral to the lesion), limb (jerky and fluttering movements of the limb contralateral to the side of the lesion), and orolingual (vacuous jaw movements and tongue protrusions) AIMs. Each of these four subtypes was scored on a severity scale from 0 to 4 (0, absent; 1, occasional; 2, frequent; 3, continuous; 4, continuous and not interruptible by outer stimuli). After L-DOPA or L-DOPA + ZNS treatment, mice were placed in separate cages and dyskinetic behaviors were assessed by AIMs scale every 20 min for 1 min, over a period of 140 min.

2.6. Surgery

A small U-frame head holder was mounted on the mouse's head to

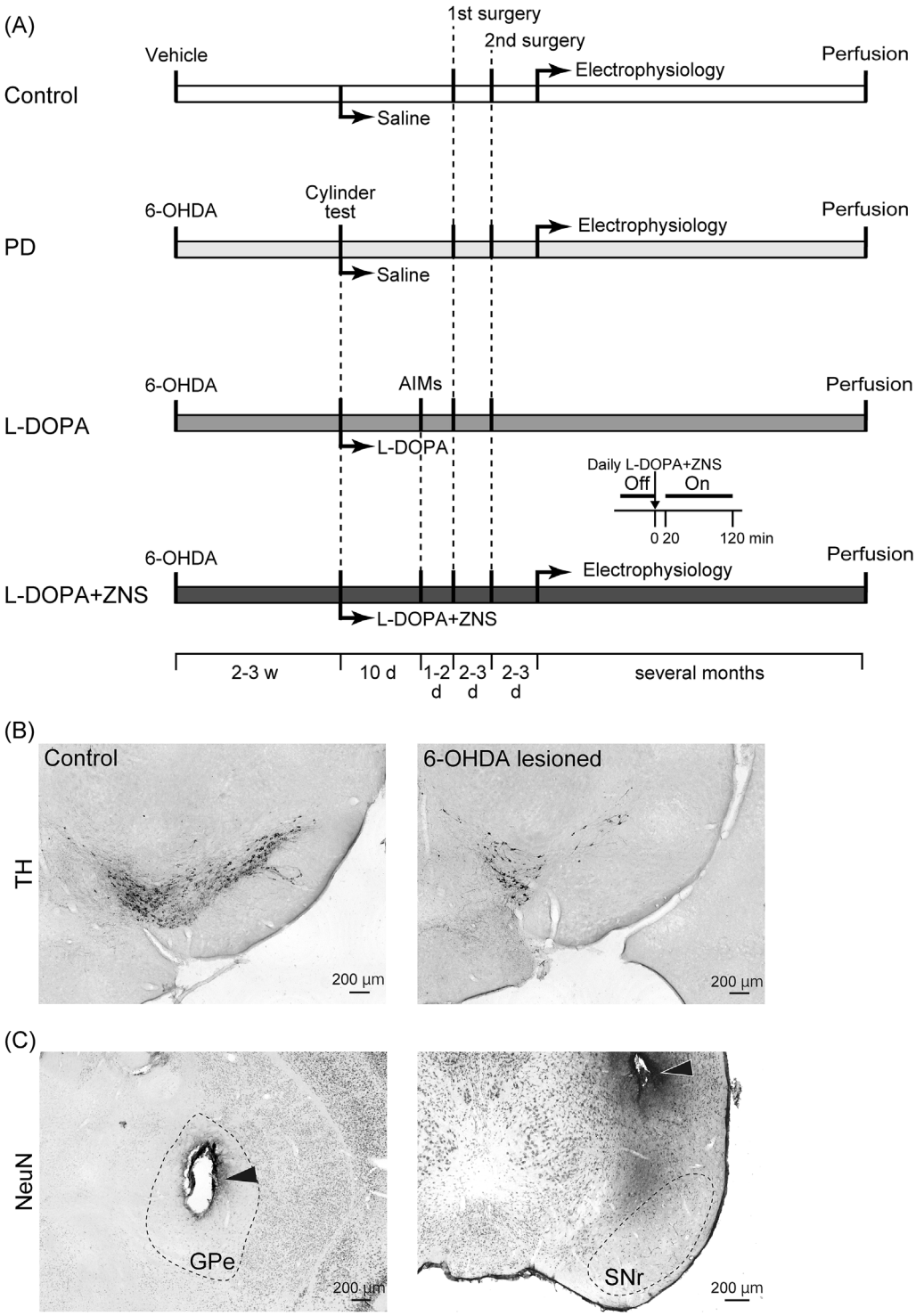

Fig. 1. Schematic representation of the experimental design and histological verifications. (A) In the beginning, mice received vehicle or 6-OHDA injection into the right medial forebrain bundle. 6-OHDA–treated mice were screened by the cylinder test after 2–3 weeks. Mice were treated daily with saline, L-DOPA, or L-DOPA + ZNS for 10 days, and AIMs were observed. Then, electrophysiological recordings in the GPe and SNr of control, PD, and L-DOPA + ZNS–treated mice were performed. In L-DOPA + ZNS–treated mice, recordings were performed before (L-DOPA + ZNS off) and 20 min after (L-DOPA + ZNS on) the daily injection of L-DOPA + ZNS. Finally, all mice were perfused transcardially and processed for histology. (B) Dopaminergic neurons in the SNc were visualized by immunostaining with TH. (C) The recording sites in the GPe (arrow head in the left panel) and SNr (arrow head in the right panel, 1 mm dorsal to the recording site). Neurons were visualized by immunostaining with NeuN.

painlessly fix the head of an awake mouse to the stereotaxic apparatus after AIMs assessment as described previously (Chiken et al., 2008; Sano et al., 2013). After recovery from this surgery (2 or 3 days later), the mouse was positioned in a stereotaxic apparatus with its head restrained using the head holder under anesthesia with isoflurane (1.0–1.5%). Parts of the skull in the right hemisphere were removed to access the motor cortex, GPe and SNr, and then two bipolar stimulating electrodes were implanted into the motor cortex (orofacial and forelimb regions) as described before (Chiken et al., 2008; Sano et al., 2013).

2.7. Recording of neuronal activity

After recovery from the second surgery, the awake mouse was positioned in a stereotaxic apparatus using the U-frame head holder. For single-unit recording in the GPe and SNr, a glass-coated tungsten microelectrode (Alpha Omega, 0.5 or 1.0 MΩ at 1 kHz) was inserted vertically into the brain through the dura mater using a hydraulic microdrive. Unit activity of GPe and SNr neurons recorded from the microelectrode was amplified and filtered (0.3–5.0 kHz), converted to digital data with a window discriminator, and sampled at 2.0 kHz using a computer for online data analysis. Spontaneous discharges and the

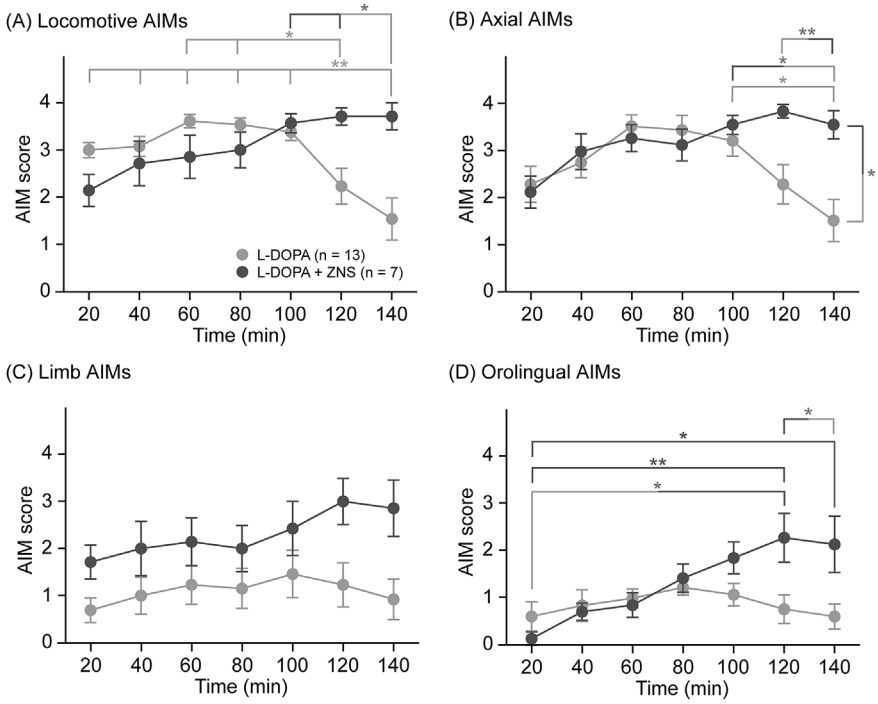

Fig. 2. ZNS increased duration and severity of LID. Locomotive (A), axial (B), limb (C), and orolingual (D) AIMs were scored at every 20 min after L-DOPA (light gray circles) or L-DOPA + ZNS (dark gray circles) administration for 140 min. Data are expressed as mean ± SEM. * $p < 0.05$, ** $p < 0.01$, significantly different between groups connected with corresponding light or dark gray lines.

responses to cortical electrical stimulation (200 μs duration, monophasic single pulse at 0.7 Hz, 20–50 μA strength) through the stimulating electrode implanted in the motor cortex were recorded. Data recorded before the daily injection of L-DOPA + ZNS were described as "L-DOPA + ZNS Off" (Fig. 1A). After the recording for "L-DOPA + ZNS Off", the awake mouse was kept in the stereotaxic apparatus and L-DOPA + ZNS was injected. Then, we recorded spontaneous discharges and the responses to cortical electrical stimulation from 20 min to 120 min after L-DOPA + ZNS injection when L-DOPA + ZNS injection induced severe LID. Data recorded after the daily injection of L-DOPA + ZNS were described as "L-DOPA + ZNS On" (Fig. 1A). After the final recording, several sites of neuronal recording were marked by passing cathodal DC current (20 μA for 20 s) through the recording electrode. Then, the mice were deeply anesthetized with sodium pentobarbital (100 mg/kg, *i.p.*) and perfused transcardially with 0.01 M PBS followed by 10% formalin in 0.01 M PBS. The brains were removed, postfixed in 10% formalin at 4 °C overnight, cryoprotected in 10% sucrose in 0.01 M PBS at 4 °C, and then in 30% sucrose in 0.01 M PBS at 4 °C.

2.8. Data analysis for neuronal activity

The spontaneous firing rate was calculated from continuous digitized recordings for 50 s. For firing pattern analysis, the interspike intervals (ISIs), the coefficient of variation (CV) of ISIs, and the burst index (a ratio of the mean ISI to the mode ISI) were calculated (Chiken et al., 2008; Sano et al., 2013). The spontaneous firing pattern was analyzed by constructing autocorrelograms (bin width of 0.5 ms) from continuous digitized recordings for 50 s.

The neuronal responses to cortical electrical stimulation were assessed by constructing peristimulus time histograms (PSTHs: bin width of 1 ms) for 100 stimulation trials. The mean value and SD of the discharge rate during the 100-ms period preceding the stimulation onset were calulated for each PSTH and considered as the basaline dischargerate. Excitation and inhibition to cortical stimulation were judged to be significant if the firing rate during at least 2 consecutive bins (2 ms) reached the statistical level of $p < 0.05$ (one-tailed *t*-test) (Chiken et al., 2008; Sano et al., 2013; Tachibana et al., 2011). The responses were judged to end when two consecutive bins fell below the significance level. The amplitude of each response was defined as the number of spikes during significant changes minus the number of spikes of the baseline discharge in the 100 stimulation trials for PSTH (positive and negative values indicate excitatory and inhibitory responses, respectively). Response patterns were classified based on the cortically evoked response. For population PSTHs, the PSTH of each neuron with significant response to motor cortical stimulation was smoothed with a Gaussian window ($\sigma = 2$ ms) and averaged.

2.9. Histology

The brains cryoprotected with 30% sucrose were frozen and sectioned coronally (40 μm). Free-floating sections were incubated with an antibody against tyrosine hydroxylase (TH; Millipore) or NeuN (Millipore), and then visualized with a biotinylated secondary antibody and the ABC method (Sano et al., 2015).

2.10. Statistical analysis

L-DOPA–induced AIMs were compared between two groups by two-way repeated measures ANOVA, and neuronal activity was compared between four groups by one-way ANOVA. Tukey's *post hoc* test was employed for multiple comparisons. Significant level was set to $p < 0.05$ or 0.01. These data analyses were performed using Prism 7 software (GraphPad Software Inc.).

3. Results

3.1. L-DOPA–induced AIMs

Injection of 6-OHDA induced dramatic decreases of TH positive neurons in the SNc (Fig. 1B). In the cylinder test, control mice showed similar usage of left and right forelimbs in wall contact. However, mice injected with 6-OHDA showed a reduction in usage of the forelimb contralateral to the lesion, and a limb use asymmetry score was decreased to 30.0%. These histological and behavioral results indicated that dopaminergic neurons were severely lesioned.

On day 10 of chronic L-DOPA or L-DOPA + ZNS treatment, AIMs were observed in different body parts and scored every 20 min for

1 min after L-DOPA or L-DOPA + ZNS treatment (Fig. 2). The locomotive AIMs scores (Fig. 2A, ANOVA: time, $p < 0.05$; treatment, $p = 0.26$; interaction, $p < 0.01$) of L-DOPA–treated mice were significantly decreased at 120 and 140 min (Tukey's *post hoc* test: 20, 40, 60, 80, and 100 min vs. 140 min, $p < 0.01$; 60 and 80 min vs. 120 min, $p < 0.05$), but those of L-DOPA + ZNS–treated mice remained high toward the end compared to L-DOPA–treated mice (Tukey's *post hoc* test: L-DOPA–treated at 140 min vs. L-DOPA + ZNS–treated at 100 and 120 min, $p < 0.05$). The axial AIMs scores (Fig. 2B, ANOVA: time, $p < 0.05$; treatment, $p < 0.05$; interaction, $p < 0.01$) of L-DOPA–-treated mice were significantly decreased at 140 min (Tukey's *post hoc* test: 100 min vs. 140 min, $p < 0.05$), but those of L-DOPA + ZNS–treated mice remained high toward the end compared to L-DOPA–treated mice (Tukey's *post hoc* test: L-DOPA + ZNS–treated at 100 min vs. L-DOPA–treated at 140 min, $p < 0.05$; L-DOPA + ZNS–treated at 140 min vs. L-DOPA–treated at 120 min, $p < 0.01$; L-DOPA + ZNS–treated at 140 min vs. L-DOPA–treated at 140 min, $p < 0.05$). The limb AIMs scores (Fig. 2C, ANOVA: time, $p = 0.57$; treatment, $p < 0.01$; interaction, $p = 0.86$) of L-DOPA + ZNS–treated mice were higher than those of L-DOPA–treated mice. The orolingual AIMs scores (Fig. 2D, ANOVA: time, $p < 0.01$; treatment, $p < 0.01$; interaction, $p < 0.01$) of L-DOPA + ZNS–treated mice significantly increased at 120 and 140 min compared to those at 20 min (Tukey's *post hoc* test: 20 min vs. 120 min, $p < 0.01$; 20 min vs. 140 min, $p < 0.05$). The orolingual AIMs scores of L-DOPA + ZNS–treated mice at 120 min were larger than those of L-DOPA–treated mice at 20 and 140 min (Tukey's *post hoc* test: L-DOPA + ZNS–treated at 120 min vs. L-DOPA–treated at 20 min, $p < 0.05$; L-DOPA + ZNS–treated at 120 min vs. L-DOPA–treated at 140 min, $p < 0.05$). Overall, L-DOPA + ZNS–treated mice showed longer and more severe AIMs than L-DOPA–treated mice. Control and PD mice without L-DOPA treatment were also observed over 140 min and never showed AIMs.

3.2. Spontaneous neuronal activity in the GPe and SNr

To elucidate the neural mechanism that underlies the finding of L-DOPA + ZNS–treated mice showing longer and more severe AIMs than L-DOPA–treated mice, we recorded spontaneous discharges in the GPe and SNr (Fig. 1C) of L-DOPA + ZNS mice in the awake state before and after L-DOPA + ZNS treatment (L-DOPA + ZNS Off and L-DOPA + ZNS On, respectively) and compared these to values from control and PD mice (Table 1, Fig. 3). In GPe neurons, there was no apparent difference in the firing rates (ANOVA: $p = 0.09$) between all groups, and the means of ISIs (ANOVA: $p < 0.05$) in L-DOPA + ZNS On were larger than those of control (Table 1). Digitized spikes and autocorrelograms showed that GPe neurons fired continuously and irregularly in all groups (Fig. 3A). The CV of ISIs (ANOVA: $p < 0.01$) and burst index (ANOVA: $p < 0.05$) in L-DOPA + ZNS Off were larger than those in the other groups (Tukey's *post hoc* test: CV of ISIs: control and L-DOPA + ZNS On vs. L-DOPA + ZNS Off, $p < 0.01$; PD vs. L-DOPA + ZNS Off, $p < 0.05$; burst index: control vs. L-DOPA + ZNS Off, $p < 0.05$; Table 1).

We also compared spontaneous activity of SNr neurons and observed an apparent difference in the firing rates (ANOVA: $p < 0.01$, Table 1) and the means of ISIs (ANOVA: $p < 0.01$, Table 1) of SNr neurons: the firing rates of L-DOPA + ZNS On were lower than those of the other groups (Tukey's *post hoc* test: control and L-DOPA + ZNS Off vs. L-DOPA + ZNS On, $p < 0.01$; PD vs. L-DOPA + ZNS On, $p < 0.05$), and the means of ISIs of L-DOPA + ZNS On were longer than those of the other groups (Tukey's *post hoc* test: control, PD, and L-DOPA + ZNS Off vs. L-DOPA + ZNS On, $p < 0.01$). The trace of digitized spikes and autocorrelograms showed that SNr neurons fired similarly to GPe neurons (Fig. 3B). The CV of ISIs (ANOVA: $p < 0.05$, Table 1) in L-DOPA + ZNS On was larger than that of control (Tukey's *post hoc* test: control vs. L-DOPA + ZNS On, $p < 0.05$) but the burst index (ANOVA: $p = 0.37$, Table 1) was comparable between all groups.

3.3. Cortically evoked responses in the GPe and SNr

We also recorded neuronal activities in the GPe and SNr (Fig. 1C) induced by motor cortical stimulation and constructed PSTHs in the L-DOPA + ZNS Off and L-DOPA + ZNS On states (Figs. 4–6, Table 2). The findings were compared to those in the control and PD states. The typical response pattern of GPe neurons evoked by electrical stimulation in the motor cortex is a triphasic response consisting of early excitation, inhibition, and late excitation in the control state (Fig. 4A), and this response pattern was major in all states (Fig. 5A). However, it seems that inhibition in L-DOPA + ZNS Off and late excitation in PD and L-DOPA + ZNS Off are increased (Fig. 4A). These changes in PD and L-DOPA + ZNS Off are evident in population PSTHs (Fig. 6A). Following this, the latency, duration, and amplitude of each component of cortically evoked responses were quantitatively analyzed (Table 2). The latency of early excitation in control and L-DOPA + ZNS On was statistically longer than that in PD (ANOVA: $p < 0.01$; Tukey's *post hoc* test, control vs. PD, $p < 0.05$; L-DOPA + ZNS On vs. PD, $p < 0.01$). The amplitude of early excitation in PD was increased compared with the other groups (ANOVA: $p < 0.01$; Tukey's *post hoc* test, control and L-DOPA + ZNS On vs. PD, $p < 0.05$; L-DOPA + ZNS Off vs. PD, $p < 0.01$). The latency of inhibition in L-DOPA + ZNS On was longer than that in control (ANOVA: $p < 0.05$; Tukey's *post hoc* test, L-DOPA + ZNS On vs. control, $p < 0.05$). The duration of inhibition in L-DOPA + ZNS Off was longer than that in control (ANOVA: $p < 0.01$; Tukey's *post hoc* test, L-DOPA+ZNS Off vs. control, $p < 0.01$). The latency of late excitation in PD, L-DOPA + ZNS Off, and L-DOPA + ZNS On was statistically longer than that of control (ANOVA: $p < 0.01$; Tukey's *post hoc* test, PD and L-DOPA + ZNS On vs. control, $p < 0.05$; L-DOPA + ZNS Off vs. control, $p < 0.01$). The duration of

Table 1
Spontaneous firing activity in the GPe and SNr.

		Control	PD	L-DOPA + ZNS Off	L-DOPA + ZNS On
GPe	No. of neurons	31	30	34	62
	Firing rate (Hz)	59.69 ± 2.69	53.81 ± 3.95	48.83 ± 3.21	48.88 ± 2.97
	ISI mean (ms)	18.39 ± 1.10*	22.19 ± 2.47	23.16 ± 1.42	25.09 ± 1.38
	CV	0.79 ± 0.07##	0.82 ± 0.042#	1.03 ± 0.05	0.68 ± 0.03##
	Burst index	1.69 ± 0.10#	2.07 ± 0.23	2.78 ± 0.35	2.01 ± 0.19
SNr	No. of neurons	20	22	31	41
	Firing rate (Hz)	51.58 ± 2.31**	44.65 ± 3.64*	52.82 ± 4.02**	32.36 ± 1.68
	ISI mean (ms)	19.93 ± 1.03**	24.42 ± 1.75**	21.58 ± 1.25**	35.43 ± 2.97
	CV	0.69 ± 0.04*	0.80 ± 0.04	0.74 ± 0.04	0.86 ± 0.05
	Burst index	1.68 ± 0.28	2.48 ± 0.36	2.99 ± 0.70	2.29 ± 0.35

Values are mean ± SEM.
*$p < 0.05$, **$p < 0.01$, significantly different from L-DOPA+ZNS On by ANOVA and Tukey's *post hoc* test.
#$p < 0.05$, ##$p < 0.01$, significantly different from L-DOPA+ZNS Off by ANOVA and Tukey's *post hoc* test.

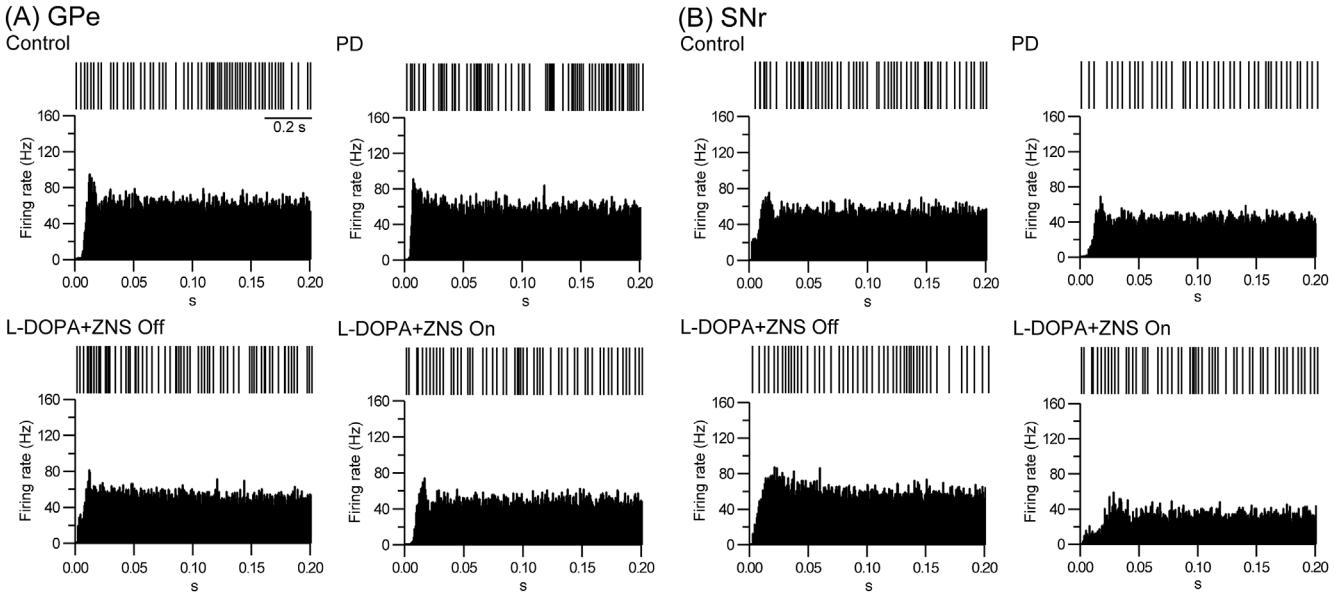

Fig. 3. No apparent effects on spontaneous activity in GPe and SNr neurons. Slow traces of digitized spikes and autocorrelograms of spontaneous activity in the GPe (A) and SNr (B) in the control, PD, L-DOPA + ZNS Off, and L-DOPA + ZNS On states.

late excitation in PD and L-DOPA + ZNS Off was apparently longer than that in L-DOPA + ZNS On (ANOVA: $p < 0.0001$; Tukey's *post hoc* test, PD and L-DOPA + ZNS Off vs. L-DOPA + ZNS On, $p < 0.01$). In addition, the duration of late excitation of L-DOPA + ZNS Off was also longer than that of control and PD (Tukey's *post hoc* test, L-DOPA + ZNS Off vs. control, $p < 0.01$; L-DOPA + ZNS Off vs. PD, $p < 0.05$). The amplitude of late excitation in L-DOPA + ZNS Off and PD was increased compared to control and L-DOPA + ZNS On (ANOVA: $p < 0.0001$; Tukey's *post hoc* test, L-DOPA + ZNS Off vs. control and L-DOPA + ZNS On, $p < 0.01$; PD vs. L-DOPA + ZNS On, $p < 0.01$).

The typical response pattern of SNr neurons evoked by electrical stimulation in the motor cortex is a triphasic response consisting of early excitation, inhibition, and late excitation in the control state (Figs. 4B and 5B). It seems that the typical response pattern in PD and L-DOPA + ZNS Off is early excitation or biphasic excitation (Figs. 4B and 5B), while that in L-DOPA + ZNS On is a triphasic response or early excitation followed by inhibition (Figs. 4B and 5B). These changes in PD, L-DOPA + ZNS Off, and L-DOPA + ZNS On were also evident in population PSTHs (Fig. 6B). The latency, duration, and amplitude of each component of cortically evoked responses were quantitatively analyzed (Table 2). The duration of early excitation in PD was significantly longer compared with the other groups (ANOVA: $p < 0.0001$; Tukey's *post hoc* test, PD vs. control and L-DOPA + ZNS On, $p < 0.01$; PD vs. L-DOPA + ZNS Off, $p < 0.05$). The amplitude of early excitation in PD was increased compared with L-DOPA + ZNS On (ANOVA: $p < 0.05$; Tukey's *post hoc* test, PD vs. L-DOPA + ZNS On, $p < 0.05$). The duration of inhibition in L-DOPA + ZNS On was apparently longer compared with the other groups (ANOVA: $p < 0.0001$; Tukey's *post hoc* test, control and PD vs. L-DOPA + ZNS On, $p < 0.01$; L-DOPA + ZNS Off vs. L-DOPA + ZNS On, $p < 0.05$). The latency of late excitation in L-DOPA + ZNS On was significantly longer than that in the other groups (ANOVA: $p < 0.0001$; Tukey's *post hoc* test, control and PD vs. L-DOPA + ZNS On, $p < 0.01$; L-DOPA + ZNS Off vs. L-

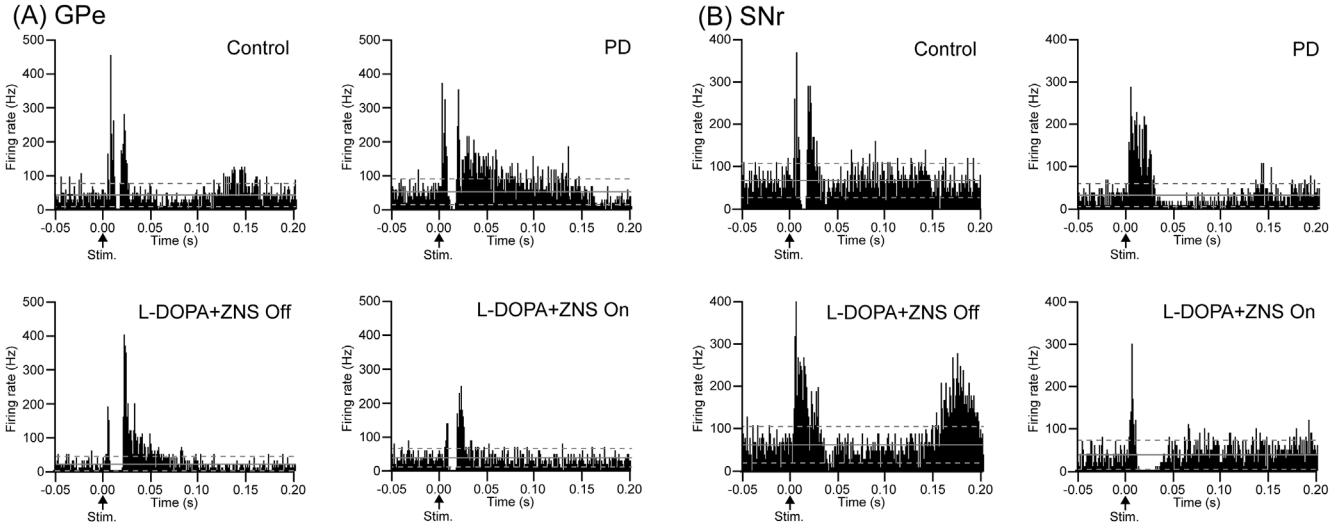

Fig. 4. Cortically evoked responses in the GPe and SNr. PSTHs of the typical response of GPe (A) and SNr (B) neurons to motor cortical stimulation in the control, PD, L-DOPA + ZNS Off, and L-DOPA + ZNS On states. Electrical stimulation (200 μs duration, single pulse, 50 μA strength) to the motor cortex was delivered at time 0 (arrows) for 100 stimulus trials. The mean firing frequency and statistical levels of $p < 0.05$ (one-tailed *t*-test) calculated from the 100 ms period preceding the onset of stimulus are indicated by solid (mean) and dotted lines (statistical levels), respectively.

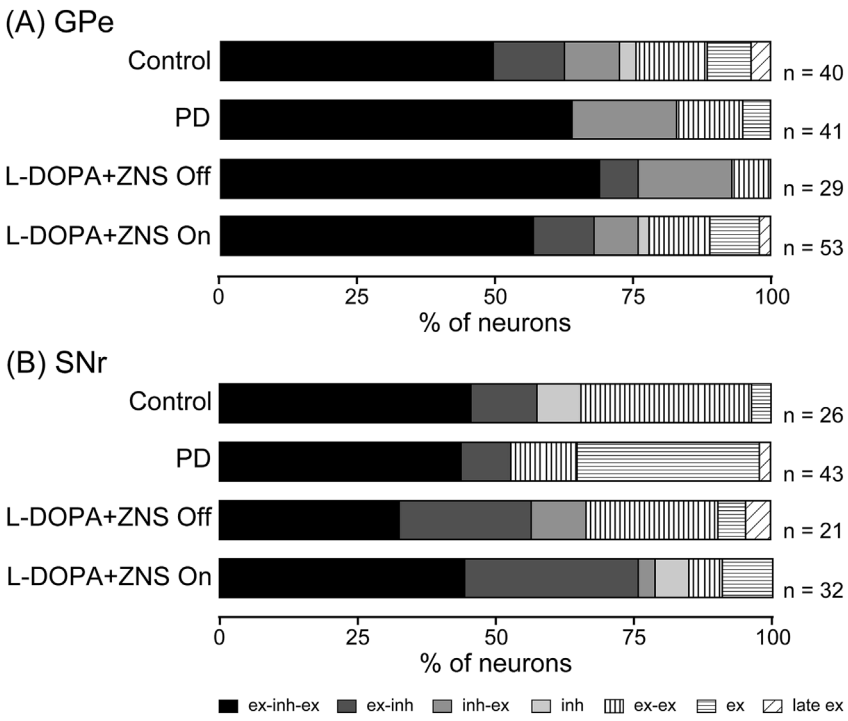

Fig. 5. Response patterns of GPe and SNr neurons to motor cortical stimulation. Proportions of GPe (A) and SNr (B) neurons classified according to the cortically evoked response patterns in the control, PD, L-DOPA + ZNS Off, and L-DOPA + ZNS On states. "ex" and "inh" indicate excitation and inhibition, respectively. "ex-inh-ex" represents a triphasic response consisting of early excitation, inhibition, and late excitation.

DOPA + ZNS On, $p < 0.05$). The duration of late excitation in PD, L-DOPA + ZNS Off, and L-DOPA + ZNS On was also clearly different from that of the control state (ANOVA: $p < 0.001$; Tukey's *post hoc* test, PD and L-DOPA + ZNS On vs. control, $p < 0.01$; L-DOPA + ZNS Off vs. control, $p < 0.05$). The amplitude of late excitation in PD, L-DOPA + ZNS Off, and L-DOPA + ZNS On was significantly smaller compared to that of control (ANOVA: $p < 0.0001$; Tukey's *post hoc* test, PD and L-DOPA + ZNS On vs. control $p < 0.01$; L-DOPA + ZNS Off vs. control, $p < 0.05$).

4. Discussion

The present study reveals the following results: (1) Chronic ZNS treatment with L-DOPA in PD model mice had no significant effect on the rate of spontaneous firing in GPe neurons. In contrast, the spontaneous firing rate of SNr neurons was decreased in the L-DOPA + ZNS On state compared with the control, PD, and L-DOPA + ZNS Off states. (2) In GPe neurons, chronic ZNS treatment with L-DOPA in PD model mice (both Off and On states) had no significant effect on cortically evoked inhibition compared with the control state. On the other hand, in SNr neurons, chronic ZNS treatment with L-DOPA (L-DOPA + ZNS On) significantly increased cortically evoked inhibition and decreased late excitation compared with the control state. (3) The L-DOPA + ZNS–treated PD model mice extended the period showing L-DOPA–induced AIMs and demonstrated more severe AIMs scores. Therefore, not only do the spontaneous firing rates of SNr neurons but also phasic signals originating from the motor cortex seem to be responsible for the increased duration and severity of L-DOPA–induced AIMs.

4.1. Effect of ZNS on spontaneous neuronal activity in the GPe and SNr

In the GPe, there was no statistical difference in the spontaneous firing rate, and little effect on the firing pattern between all groups (Table 1). However, the firing rate in SNr neurons was decreased in L-DOPA + ZNS On compared with control, PD, and L-DOPA + ZNS Off (Table 1). According to the classical model of the basal ganglia (DeLong, 1990), the *direct* pathway inhibits the SNr/EPN, and disinhibition of the thalamus facilitates movements. On the contrary, the *indirect* pathway activates the SNr/EPN and causes inhibition of the thalamus, which decreases movements. This model predicts an excessive activation of SNr/EPN neurons in the parkinsonian state and their hypoactivity in LID (Obeso et al., 2000). It was shown that the firing rate in the SNr was increased in L-DOPA–treated PD model rats

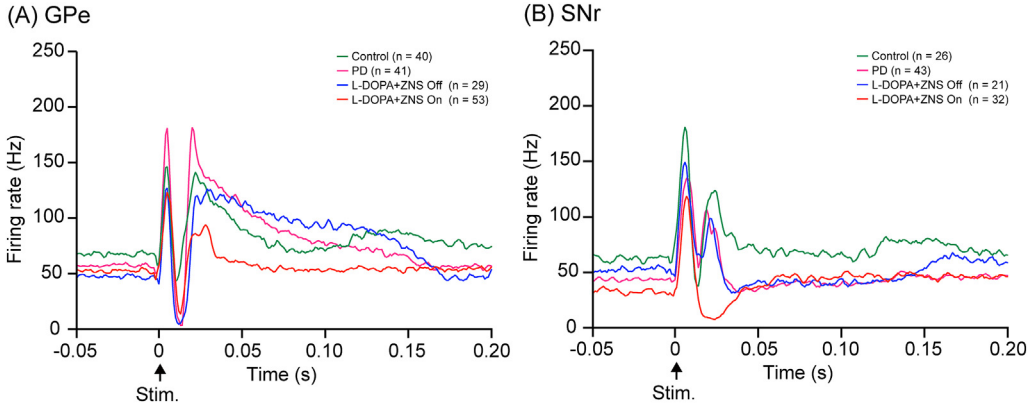

Fig. 6. Changes in the population PSTHs of GPe and SNr neurons. Population PSTHs of GPe (A) and SNr (B) neurons in the control (green lines), PD (pink), L-DOPA + ZNS Off (blue), and L-DOPA + ZNS On (red) states. Numbers of neurons used are indicated by n. (For interpretation of the references to colour in this figure legend, the reader is referred to the Web version of this article.)

Table 2
Cortically evoked response parameters in the GPe and SNr.

		Control	PD	L-DOPA + ZNS Off	L-DOPA + ZNS On
GPe	No. of neurons	40	41	29	53
	Early excitation	n = 33	n = 34	n = 24	n = 47
	Latency (ms)	4.36 ± 0.35	3.12 ± 0.21**$	3.58 ± 0.22	4.70 ± 0.36
	Duration (ms)	3.30 ± 0.35	3.98 ± 0.39	3.10 ± 0.35	3.49 ± 0.28
	Amplitude (spikes)	39.33 ± 4.74	60.95 ± 6.68*##$	35.06 ± 4.87	40.27 ± 3.99
	Inhibition	n = 30	n = 38	n = 27	n = 42
	Latency (ms)	9.33 ± 0.44*	10.05 ± 0.29	9.63 ± 0.49	10.98 ± 0.38
	Duration (ms)	5.05 ± 0.58##	7.52 ± 0.76	8.90 ± 0.77	6.98 ± 0.77
	Amplitude (spikes)	−34.20 ± 4.64	−40.16 ± 4.49	−40.76 ± 4.35	−31.72 ± 3.44
	Late excitation	n = 31	n = 41	n = 27	n = 41
	Latency (ms)	16.97 ± 0.70*	21.27 ± 1.14$	24.00 ± 1.46$$	21.20 ± 0.72$
	Duration (ms)	26.10 ± 8.20##	39.74 ± 5.67**#	66.38 ± 10.36**	6.51 ± 0.98
	Amplitude (spikes)	224.00 ± 58.48##	388.20 ± 69.35**	584.20 ± 99.81	62.22 ± 11.17##
SNr	No. of neurons	26	43	21	32
	Early excitation	n = 24	n = 41	n = 18	n = 29
	Latency (ms)	4.08 ± 0.38	4.34 ± 0.33	5.06 ± 0.77	4.90 ± 0.40
	Duration (ms)	5.19 ± 0.57	11.00 ± 1.29**#$$	6.24 ± 1.16	5.28 ± 0.71
	Amplitude (spikes)	69.21 ± 11.34	124.9 ± 17.77*	82.00 ± 12.9	68.47 ± 12.92
	Inhibition	n = 17	n = 23	n = 14	n = 27
	Latency (ms)	11.24 ± 0.63	13.09 ± 0.54	15.86 ± 2.61	15.07 ± 1.01
	Duration (ms)	6.15 ± 1.29**	4.61 ± 0.94**	10.43 ± 3.45*	18.88 ± 2.50
	Amplitude (spikes)	−37.85 ± 8.00	−21.29 ± 4.35	−51.86 ± 25.14	−49.93 ± 6.8
	Late excitation	n = 20	n = 25	n = 15	n = 17
	Latency (ms)	18.95 ± 1.05**	22.68 ± 1.42**	28.33 ± 8.98*	48.06 ± 3.80
	Duration (ms)	12.15 ± 2.92	3.88 ± 0.74$$	4.43 ± 1.05$	4.69 ± 1.15$$
	Amplitude (spikes)	127.60 ± 31.06	40.77 ± 7.44$$	54.70 ± 12.07$	21.33 ± 4.96$$

Values are mean ± SEM. Neurons with significant early excitation, inhibition, and late excitation were used for calculation (n indicates number of neurons used).
*$p < 0.05$, **$p < 0.01$, significantly different from L-DOPA + ZNS On by ANOVA and Tukey's *post hoc* test.
#$p < 0.05$, ##$p < 0.01$, significantly different from L-DOPA + ZNS Off by ANOVA and Tukey's *post hoc* test.
\$$p < 0.05$, \$\$$p < 0.01$, significantly different from control by ANOVA and Tukey's *post hoc* test.

compared to control and decreased after an acute challenge of L-DOPA to the same rats (Aristieta et al., 2016). Therefore, it is reasonable to assume that the reduction of the firing rate in the SNr in L-DOPA + ZNS On is related to the appearance of AIMs. MPTP–induced parkinsonian monkeys, on the other hand, failed to show an expected increase in output nuclei of the basal ganglia (Tachibana et al., 2011; Wichmann et al., 1999). These previous and current data suggest that the spontaneous activity of the output nuclei of the basal ganglia has a limited effect on the regulation of motor control. Even if the spontaneous activity of SNr neurons might have a limited effect on PD and LID symptoms, chronic ZNS treatment can decrease spontaneous activity of SNr neurons in the L-DOPA + ZNS On state and induce AIMs.

4.2. Effect of ZNS on cortically evoked responses in the GPe and SNr

The basal ganglia receive massive projections from the cerebral cortex. To elucidate the functions of the basal ganglia, it is essential to investigate information processing along the cortico-basal ganglia circuit. Previous studies showed that electrical stimulation to the motor cortex mainly evoked a triphasic response pattern consisting of early excitation, inhibition, and late excitation in the GPe, SNr, and EPN of rodents (Chiken et al., 2008, 2015; Fujimoto and Kita, 1992; Sano et al., 2013) and in the GPe, internal segment of the globus pallidus (GPi, corresponding to the EPN), and SNr of monkeys (Iwamuro et al., 2017; Kitano et al., 1998; Yoshida et al., 1993). The responsible pathways for each component were investigated. Cortically evoked early excitation in the GPe and SNr is considered to be mediated by the cortico-STN-GPe and cortico-STN-SNr *hyperdirect* pathways, respectively (Inoue et al., 2012; Nambu et al., 2000). Cortically evoked inhibition in the GPe and SNr is mediated by the cortico-striato-GPe and cortico-striato-SNr *direct* pathways, respectively (Sano et al., 2013; Tachibana et al., 2008). Cortically evoked late excitation in the GPe and SNr is derived from the cortico-striato-GPe-STN-GPe and cortico-striato-GPe-STN-SNr *indirect* pathways, respectively (Sano et al., 2013; Tachibana et al., 2008).

In the current study, all groups showed cortically evoked triphasic response patterns consisting of early excitation, inhibition, and late excitation as the typical response pattern in the GPe (Figs. 4A and 5A). Chronic ZNS + L-DOPA treatment showed comparable inhibition in the GPe compared to the control state in the On state (L-DOPA + ZNS On). Cortically evoked inhibition of GPe neurons is considered to be mediated by the cortico-striato-GPe pathway, therefore, we assume that chronic ZNS treatment in the On state (L-DOPA + ZNS On) affects the neuronal trunsduction through the cortico-striato-GPe pathway to return to the control state. Chronic ZNS + L-DOPA treatment also increased cortically evoked late excitation of GPe neurons in the Off state (L-DOPA + ZNS Off) compared to the control and L-DOPA + ZNS On states (Figs. 4A and 6A, Table 2). The cortically evoked late excitation of GPe neurons is considered to be derived from the cortico-striato-GPe-STN-GPe pathway, and the neuronal transduction through this pathway was probably facilitated in the L-DOPA + ZNS Off state compared with the L-DOPA + ZNS On state. The L-DOPA + ZNS On state may normalize the cortico-striato-GPe-STN-GPe transduction.

In the SNr, the typical cortically evoked response pattern is a triphasic response consisting of early excitation, inhibition, and late excitation in the control state. In the PD and L-DOPA + ZNS Off states, the typical response pattern is monophasic excitation or biphasic excitation, while triphasic response or biphasic response consisting of early excitation followed by inhibition is the major response pattern in the L-DOPA + ZNS On state (Figs. 4B and 5B). Chronic ZNS + L-DOPA treatment significantly increased cortically evoked inhibition in the SNr in the On state (L-DOPA + ZNS On) compared to the control, PD, and L-DOPA + ZNS Off states (Figs. 4B and 6B, Table 2). Cortically evoked late

excitation of SNr neurons was significantly decreased in the PD, L-DOPA + ZNS Off, and L-DOPA + ZNS On states compared with the control state (Figs. 4B and 6B, Table 2). Cortically evoked inhibition was decreased, and early excitation and late excitation were probably fused and judged as monophasic excitation in some responses of the SNr neurons in PD and L-DOPA + ZNS Off. As a result, late excitation of SNr neurons in PD and L-DOPA + ZNS Off looks to be decreased, and we think that late excitation in the SNr is not necessarily decreased. On the other hand, cortically evoked inhibition was facilitated in the L-DOPA + ZNS On state. Therefore, we assume that cortically evoked late excitation of SNr neurons in L-DOPA + ZNS On is indeed significantly decreased. The cortically evoked inhibition and late excitation of SNr neurons are considered to be mediated by the cortico-striato-SNr *direct* and cortico-striato-GPe-STN-SNr *indirect* pathways, respectively. We propose that the neuronal transduction through the *direct* pathway is decreased in the PD and L-DOPA + ZNS Off states; on the other hand, that of the *direct* pathway is facilitated, and that of the *indirect* pathway is reduced in the L-DOPA + ZNS On state.

4.3. Effect of ZNS on the basal ganglia in LID

In the current model of the basal ganglia, three parallel pathways, i.e., *direct*, *indirect,* and *hyperdirect* pathways, connect the input stations and output nuclei of the basal ganglia. These three pathways are considered to exert different effects on output nuclei (SNr/EPN) and control movements. The *direct* pathway decreases the activity in the SNr/EPN and facilitates movements by disinhibition of thalamocortical activity; on the other hand, the *indirect* and *hyperdirect* pathways increase the activity in the SNr/EPN and suppress movements by inhibition of thalamocortical activity. The dynamic model version of the basal ganglia was also proposed as follows (Mink and Thach, 1993; Nambu et al., 2002). First, the *hyperdirect* pathway excites the SNr/EPN and resets cortical activity. Second, the *direct* pathway inhibits the SNr/EPN and releases appropriate movements. Finally, the *indirect* pathway excites the SNr/EPN again and induces a clear termination of the movement released by the *direct* pathway. This model can be used to explain the effect of ZNS in LID: In the PD and L-DOPA + ZNS Off states, cortically evoked inhibition in the SNr is diminished, and movements cannot be released, resulting in akinesia. On the other hand, in the L-DOPA + ZNS On state, cortically evoked inhibition is facilitated, and cortically evoked late excitation is diminished in the SNr. This condition facilitates the release of movements and inhibits the termination of movements, resulting in AIMs.

Although ZNS improves motor functions in PD (Murata et al., 2007, 2016), the precise mechanism of action is not fully understood. Based on the present study, ZNS most likely has effects on both the *direct* and *indirect* pathways. ZNS depressed the current-evoked repetitive firing discharge in striatal projection neurons and the amplitude of cortico-striatal glutamatergic transmission *in vitro* (Costa et al., 2010). ZNS was also reported as a T-type Ca^{2+} channel blocker and inhibited the low-voltage-activated Ca^{2+} current in STN neurons (Yang et al., 2014). These effects on the *indirect* pathway probably cause changes in cortically evoked late excitation in the SNr. In addition, the expression level of the D1 receptor was increased in L-DOPA and L-DOPA + ZNS–treated PD model rats, although adenosine A2A receptor expression was increased only in L-DOPA–treated PD model rats (Oki et al., 2017). These changes in mRNA expression suggest that signals through D1 and A2A receptors are facilitated in the *direct* and *indirect* pathways, respectively. Therefore, we assume that cortically evoked inhibition in the L-DOPA + ZNS On state is increased through D1 signaling in the *direct* pathway.

In the present study, we failed to show that ZNS ameliorates LID in PD (Oki et al., 2017) but rather that it facilitates the duration and severity of LID as evidenced by the behavioral and neurophysiological results. The difference of the results between these studies may be caused by the difference of ZNS dose (52 mg/kg, twice daily [(Oki et al., 2017)] vs. 100 mg/kg once daily in this study). ZNS may amplify the effects of L-DOPA both in PD and in LID, resulting in longer and more severe LID. However, ZNS can reduce the daily dose of L-DOPA, and ultimately delay the appearance of LID during long-term L-DOPA therapy in the clinical setting.

Conflicts of interest

This study was partly supported by a Research Grant from Sumitomo Dainippon Pharma Co., Ltd.

Acknowledgements

This work was partially supported by JSPS KAKENHI Grant Number JP16K01968 (to H.S.) and JP26250009 (to A.N.), MEXT KAKENHI Grant Number JP15H01458, JP17H05590 (Adaptive Circuit Shift) (to H.S.), and JP15H05873 (Non-linear Neuro-oscillology) (to A.N.), and a Research Grant from Sumitomo Dainippon Pharma Co., Ltd. (to A.N.). We also thank S. Sato, N. Suzuki, M. Goto, K. Awamura, and R. Kageyama for technical assistance.

References

Alexander, G., Crutcher, M., 1990. Functional architecture of basal ganglia. Trend. Neurosci. 13, 266–271.
Aristieta, A., Ruiz-Ortega, J.A., Miguelez, C., Morera-Herreras, T., Ugedo, L., 2016. Chronic L-DOPA administration increases the firing rate but does not reverse enhanced slow frequency oscillatory activity and synchronization in substantia nigra pars reticulata neurons from 6-hydroxydopamine-lesioned rats. Neurobiol. Dis. 89, 88–100.
Asanuma, M., Miyazaki, I., Diaz-Corrales, F.J., Kimoto, N., Kikkawa, Y., Takeshima, M., Miyoshi, K., Murata, M., 2010. Neuroprotective effects of zonisamide target astrocyte. Ann. Neurol. 67, 239–249.
Chiken, S., Shashidharan, P., Nambu, A., 2008. Cortically evoked long-lasting inhibition of pallidal neurons in a transgenic mouse model of dystonia. J. Neurosci. 28, 13967–13977.
Chiken, S., Sato, A., Ohta, C., Kurokawa, M., Arai, S., Maeshima, J., Sunayama-Morita, T., Sasaoka, T., Nambu, A., 2015. Dopamine D1 receptor-mediated transmission maintains information flow through the cortico-striato-entopeduncular direct pathway to release movements. Cerebr. Cortex 25, 4885–4897.
Choudhury, M.E., Moritoyo, T., Yabe, H., Nishikawa, N., Nagai, M., Kubo, M., Matsuda, S., Nomoto, M., 2010. Zonisamide attenuates MPTP neurotoxicity in marmosets. J. Pharmacol. Sci. 114, 298–303.
Costa, C., Tozzi, A., Luchetti, E., Siliquini, S., Belcastro, V., Tantucci, M., Picconi, B., Ientile, R., Calabresi, P., Pisani, F., 2010. Electrophysiological actions of zonisamide on striatal neurons: selective neuroprotection against complex I mitochondrial dysfunction. Exp. Neurol. 221, 217–224.
DeLong, M.R., 1990. Primate models of movement disorders of basal ganglia origin. Trends Neurosci. 13, 281–285.
Franklin, K.B.J., Paxinos, G., 2013. Paxinos and Franklin's the Mouse Brain in Stereotaxic Coordinates, fourth ed. Academic Press, an imprint of Elsevier, Amsterdam.
Fujimoto, K., Kita, H., 1992. Responses of rat substantia nigra pars reticulata units to cortical stimulation. Neurosci. Lett. 142, 105–109.
Inoue, K., Koketsu, D., Kato, S., Kobayashi, K., Nambu, A., Takada, M., 2012. Immunotoxin-mediated tract targeting in the primate brain: selective elimination of the cortico-subthalamic "hyperdirect" pathway. PLoS One 7, e39149.
Iwamuro, H., Tachibana, Y., Ugawa, Y., Saito, N., Nambu, A., 2017. Information processing from the motor cortices to the subthalamic nucleus and globus pallidus and their somatotopic organizations revealed electrophysiologically in monkeys. Eur. J. Neurosci. 46, 2684–2701.
Jankovic, J., 2008. Parkinson's disease: clinical features and diagnosis. J. Neurol. Neurosurg. Psychiatry 79, 368–376.
Jenner, P., 2008. Molecular mechanisms of L-DOPA-induced dyskinesia. Nat. Rev. Neurosci. 9, 665–677.
Kitano, H., Tanibuchi, I., Jinnai, K., 1998. The distribution of neurons in the substantia nigra pars reticulata with input from the motor, premotor and prefrontal areas of the cerebral cortex in monkeys. Brain Res. 784, 228–238.
Kito, M., Maehara, M., Watanabe, K., 1996. Mechanisms of T-type calcium channel blockade by zonisamide. Seizure 5, 115–119.
Lundblad, M., Andersson, M., Winkler, C., Kirik, D., Wierup, N., Cenci, M.A., 2002. Pharmacological validation of behavioural measures of akinesia and dyskinesia in a rat model of Parkinson's disease. Eur. J. Neurosci. 15, 120–132.
Lundblad, M., Vaudano, E., Cenci, M.A., 2003. Cellular and behavioural effects of the adenosine A2a receptor antagonist KW-6002 in a rat model of l-DOPA-induced dyskinesia. J. Neurochem. 84, 1398–1410.
Lundblad, M., Picconi, B., Lindgren, H., Cenci, M.A., 2004. A model of L-DOPA-induced dyskinesia in 6-hydroxydopamine lesioned mice: relation to motor and cellular parameters of nigrostriatal function. Neurobiol. Dis. 16, 110–123.
Lundblad, M., Usiello, A., Carta, M., Hakansson, K., Fisone, G., Cenci, M.A., 2005.

Pharmacological validation of a mouse model of l-DOPA-induced dyskinesia. Exp. Neurol. 194, 66–75.
Meredith, G.E., Kang, U.J., 2006. Behavioral models of Parkinson's disease in rodents: a new look at an old problem. Mov. Disord. 21, 1595–1606.
Mink, J.W., Thach, W.T., 1993. Basal ganglia intrinsic circuits and their role in behavior. Curr. Opin. Neurobiol. 3, 950–957.
Murata, M., Horiuchi, E., Kanazawa, I., 2001. Zonisamide has beneficial effects on Parkinson's disease patients. Neurosci. Res. 41, 397–399.
Murata, M., 2004. Novel therapeutic effects of the anti-convulsant, zonisamide, on Parkinson's disease. Curr. Pharmaceut. Des. 10, 687–693.
Murata, M., Hasegawa, K., Kanazawa, I., 2007. Zonisamide improves motor function in Parkinson disease: a randomized, double-blind study. Neurology 68, 45–50.
Murata, M., Hasegawa, K., Kanazawa, I., Fukasaka, J., Kochi, K., Shimazu, R., Japan Zonisamide on, P.D.S.G., 2015. Zonisamide improves wearing-off in Parkinson's disease: a randomized, double-blind study. Mov. Disord. 30, 1343–1350.
Murata, M., Hasegawa, K., Kanazawa, I., Shirakura, K., Kochi, K., Shimazu, R., 2016. Randomized placebo-controlled trial of zonisamide in patients with Parkinson's disease. Neurol. Clin. Neurosci. 4, 10–15.
Nambu, A., Tokuno, H., Hamada, I., Kita, H., Imanishi, M., Akazawa, T., Ikeuchi, Y., Hasegawa, N., 2000. Excitatory cortical inputs to pallidal neurons via the subthalamic nucleus in the monkey. J. Neurophysiol. 84, 289–300.
Nambu, A., Tokuno, H., Takada, M., 2002. Functional significance of the cortico-subthalamo-pallidal 'hyperdirect' pathway. Neurosci. Res. 43, 111–117.
Obeso, J.A., Oroz, R.O., M R L, L.J., J A, N., G C, W.O., 2000. Pathophysiology of the basal ganglia in Parkinson's disease. Trend. Neurosci. 23, S8–S19.
Okada, M., Kaneko, S., Hirano, T., Mizuno, K., Kondo, T., Otani, K., Fukushima, Y., 1995. Effects of zonisamide on dopaminergic system. Epilepsy Res. 22, 193–205.
Oki, M., Kaneko, S., Morise, S., Takenouchi, N., Hashizume, T., Tsuge, A., Nakamura, M., Wate, R., Kusaka, H., 2017. Zonisamide ameliorates levodopa-induced dyskinesia and reduces expression of striatal genes in Parkinson model rats. Neurosci. Res. 122, 45–50.
Peters, D.H., Sorkin, E.M., 1993. Zonisamide. A review of its pharmacodynamic and pharmacokinetic properties, and therapeutic potential in epilepsy. Drugs 45, 760–787.
Sano, H., Chiken, S., Hikida, T., Kobayashi, K., Nambu, A., 2013. Signals through the striatopallidal indirect pathway stop movements by phasic excitation in the substantia nigra. J. Neurosci. 33, 7583–7594.
Sano, H., Murata, M., Nambu, A., 2015. Zonisamide reduces nigrostriatal dopaminergic neurodegeneration in a mouse genetic model of Parkinson's disease. J. Neurochem. 134, 371–381.
Schallert, T., Fleming, S.M., Leasure, J.L., Tillerson, J.L., ST, B., 2000. CNS plasticity and assessment of forelimb sensorimotor outcome in unilateral rat models of stroke, cortical ablation, parkinsonism and spinal cord injury. Neuropharmacology 39, 777–787.
Seino, M., 2004. Review of zonisamide development in Japan. Seizure 13 (Suppl. 1), S2–S4.
Sobieszek, G., Borowicz, K.K., Kimber-Trojnar, Z., Malek, R., Piskorska, B., Czuczwar, S.J., 2003. Zonisamide: a new antiepileptic drug. Pol. J. Pharmacol. 55, 683–689.
Suzuki, S., Kawakami, K., Nishimura, S., Watanabe, Y., Yagi, K., Seino, M., Miyamoto, K., 1992. Zonisamide blocks T-type calcium channel in cultured neurons of rat cerebral cortex. Epilepsy Res. 12, 21–27.
Tachibana, Y., Kita, H., Chiken, S., Takada, M., Nambu, A., 2008. Motor cortical control of internal pallidal activity through glutamatergic and GABAergic inputs in awake monkeys. Eur. J. Neurosci. 27, 238–253.
Tachibana, Y., Iwamuro, H., Kita, H., Takada, M., Nambu, A., 2011. Subthalamo-pallidal interactions underlying parkinsonian neuronal oscillations in the primate basal ganglia. Eur. J. Neurosci. 34, 1470–1484.
Tillerson, J.L., Cohen, A.D., Philhower, J., Miller, G.W., Zigmond, M.J., T, S., 2001. Forced limb-use effects on the behavioral and neurochemical effects of 6-hydroxydopamine. J. Neurosci. 21, 4427–4435.
Wichmann, T., Bergman, H., Starr, P.A., Subramanian, T., Watts, R.L., DeLong, M.R., 1999. Comparison of MPTP-induced changes in spontaneous neuronal discharge in the internal pallidal segment and in the substantia nigra pars reticulata in primates. Exp. Brain Res. 125, 397–409.
Yang, Y.C., Tai, C.H., Pan, M.K., Kuo, C.C., 2014. The T-type calcium channel as a new therapeutic target for Parkinson's disease. Pflügers Archiv 466, 747–755.
Yano, R., Yokoyama, H., Kuroiwa, H., Kato, H., Araki, T., 2009. A novel anti-Parkinsonian agent, zonisamide, attenuates MPTP-induced neurotoxicity in mice. J. Mol. Neurosci. 39, 211–219.
Yoshida, S., Nambu, A., Jinnai, K., 1993. The distribution of the globus pallidus neurons with input from various cortical areas in the monkeys. Brain Res. 611, 170–174.